


SLC25A22 Promotes Proliferation and Metastasis of Osteosarcoma Cells via the PTEN Signaling Pathway

Technology in Cancer Research & Treatment
 Volume 17: 1-10
 © The Author(s) 2018
 Article reuse guidelines:
sagepub.com/journals-permissions
 DOI: 10.1177/1533033818811143
journals.sagepub.com/home/tct


Ming-Wei Chen, PhD¹ and Xue-jian Wu, PhD¹ 

Abstract

Osteosarcoma is a highly malignant bone tumor. However, due to the high complexity of the occurrence and metastasis of osteosarcoma, the exact mechanism promoting its development and progression remains to be elucidated. This study highlights the causal link between solute carrier family 25 member 22 (SLC25A22) and the development, progression, and metastasis of osteosarcoma. SLC25A22 is upregulated in human osteosarcoma and predicts a poor prognosis. The upregulation of SLC25A22 in osteosarcoma tissues was significantly associated with cell proliferation, invasion, and metastasis. Studies of functional gain (overexpression) and loss (knockdown) showed that SLC25A22 significantly increases the ability of osteosarcoma cells to proliferate, as well as invade and metastasize *in vitro*. At the same time, the expression of SLC25A22 promoted the progression of the cell cycle of osteosarcoma cell lines and inhibited the apoptosis of osteosarcoma cells. Analysis using a mouse xenograft model showed that xenografts of SLC25A22 stable overexpressing osteosarcoma cells had a significant increase in tumor volume and weight compared to the control group. Lung metastasis models in mice showed that expression of SLC25A22 promoted lung metastasis of osteosarcoma *in vivo*. Furthermore, SLC25A22 inhibited phosphatase and tensin homolog expression and increased phosphorylation of protein kinase b (Akt) and Focal Adhesion Kinase (FAK) in the phosphatase and tensin homolog signaling pathway. In summary, SLC25A22 is highly expressed in osteosarcoma, promoting osteosarcoma cell proliferation and invasion by inhibiting the phosphatase and tensin homolog signaling pathway.

Keywords

SLC25A22, osteosarcoma, proliferation, metastasis, PTEN signaling pathway

Abbreviations

CDK4, cyclin-dependent kinase 4; EMT, epithelial to mesenchymal transition; IHC, immunohistochemical; MDM2, mouse double minute 2; PCNA, proliferating cell nuclear antigen; PTEN, phosphatase and tensin homolog; Rb, retinoblastoma; RT-PCR, Reverse transcriptase-polymerase chain reaction.

Received: June 24, 2018; Revised: August 4, 2018; Accepted: August 31, 2018.

Introduction

Osteosarcoma is the most common primary bone malignancy in children and adolescents, with an annual incidence of approximately 4 per 100 million.¹⁻³ Prior to 1970, the 5-year survival rate was less than 20% for the treatment of limbless osteosarcoma without amputation,⁴ with the main cause of morbidity being lung metastasis. Despite numerous studies conducted by many international research institutions, the survival rate of bone remains the same.⁵ After considerable progress in magnetic resonance imaging, limb salvage surgery, and neoadjuvant chemotherapy, the clinical diagnosis, and treatment of

osteosarcoma has once again plateaued.^{6,7} The mechanisms of cell proliferation, metastasis, and neovascularization of osteosarcoma are extremely complex, involving many signal

¹ Orthopedics department, The First Affiliated Hospital of Zhengzhou University, Zhengzhou, Henan province, China

Corresponding Author:

Xue-jian Wu, PhD, Orthopedics department, The First Affiliated Hospital of Zhengzhou University, No.1 Jianshe East Road, Zhengzhou 450052, Henan province, China.
 Email: wxj20181130@163.com



transduction pathways. An in-depth understanding of the pathogenesis of osteosarcoma, new therapeutic drugs and approaches, as well as further improvement in prognosis are still required.⁸

The p53 gene and retinoblastoma (Rb) inhibitory genes play an important role in the pathogenesis of osteosarcoma.⁹⁻¹¹ In osteosarcoma, mouse double minute 2 (MDM2) and cyclin-dependent kinase 4 (CDK4) are frequently amplified or over-expressed, and MDM2 gene products can interact with p53 protein. In combination with inactivation, the CDK4 product is a cyclin-dependent protein kinase that easily inactivates Rb function,^{12,13} which may be its tumorigenic mechanism. Inhibition of tyrosine kinase signaling is a key area of targeted therapy for osteosarcoma.¹⁴ Tyrosine kinase inhibitors can competitively block tyrosine kinase receptors or bind directly to it to block the signal transduction pathway.

Phosphatase and tensin homolog (PTEN) encodes a variety of special proteins that regulate cellular biological processes such as cell growth, proliferation, and migration, including inhibition of the progression of certain tumor cell cycles and promotion of apoptosis.^{15,16} Studies found that the occurrence, development, and prognosis of various human tumors such as glioma, breast cancer, prostate cancer, leukemia, and gastrointestinal tumors may be related to the abnormal expression of *PTEN* gene.¹⁷⁻¹⁹ Down-regulation of *PTEN* gene expression and loss of function may play an important role in the development of multiple malignancies. Deletion of the *PTEN* gene is also found in osteosarcoma, and the positive expression rate of PTEN in osteosarcoma is significantly lower than that in adjacent tissues.²⁰ But whether the abnormal expression of PTEN plays a direct role in the occurrence and development of osteosarcoma and the molecular mechanism of this effect is not yet clear.

SLC25A22 is a member of the mitochondrial transporter family that facilitates the transport of glutamate across the inner mitochondrial membrane into the mitochondrial matrix.^{21,22} In previous studies, SLC25A22 has a tumor-promoting function, promoting proliferation and migration of colorectal cancer cells with mutant KRAS, and formation and metastasis of colorectal cancer xenograft tumors in mice. Patients with colorectal tumors that express increased levels of SLC25A22 have shorter survival times than patients whose tumors have lower levels. SLC25A22 induces intracellular synthesis of aspartate, activation of mitogen-activated protein kinase and extracellular signal-regulated kinase signaling and reduces oxidative stress.^{23,24} However, the role of SLC25A22 in tumor growth and metastasis regulation in osteosarcoma has not been fully elucidated. In this study, we investigated the biological effect, mechanistic action, and clinical implications of SLC25A22 in osteosarcoma.

Materials and Methods

Cell Lines and Materials

The U2OS, Saos-2, and HOS cell lines were purchased from ATCC and cultured in DMEM (Gibco, USA) supplemented with

10% FBS (Gibco, USA). The antibodies SLC25A22 (Abcam, ab137614, England), Cdc25c (Cell Signaling Technology, 4688, USA), Bcl-2 (Cell Signaling Technology, 15071, USA), cleaved caspase-3 (Cell Signaling Technology, 9664, USA), cleaved caspase-9 (Cell Signaling Technology, 9505, USA), cleaved PARP (Abcam, ab32064, England), cyclin D1 (Cell Signaling Technology, 2922, USA), cyclin B1 (Cell Signaling Technology, 4138, USA), Bad (Abcam, ab90435, England), E-cadherin (Cell Signaling Technology, 3195, USA), vimentin (Cell Signaling Technology, 5741, USA), MMP-9 (Cell Signaling Technology, 13667, USA), PTEN (Cell Signaling Technology, 9188, USA), p-Akt (Cell Signaling Technology, 4060, USA), p-FAK (Abcam, ab81298, England), and glyceraldehyde-3-phosphate dehydrogenase (GAPDH) (Cell Signaling Technology, 2118, USA) were used. FITC-Annexin V and PE-propidium iodide (PE-PI) reagents were purchased from Sigma-Aldrich (APOAF).

Immunohistochemistry

All osteosarcoma samples originated from the First Affiliated Hospital of Zhengzhou University. Paraformaldehyde-fixed osteosarcoma tissue samples were paraffin-embedded and sectioned. The sections were deparaffinized in xylene, quenched with hydrogen peroxide, then rehydrated with ethanol and antigen-recovered and blocked in sodium citrate buffer. Sections were incubated with SLC25A22 antibodies for 1 hour at room temperature, prior to incubation with secondary Horseradish Peroxidase (HRP)-polymerized antibodies, visualized with DAB, and counterstained with hematoxylin. The staining intensity and percentage of stained cells was then assessed. The immunohistochemical staining was evaluated by semi-quantitative methods, including staining intensity (0-negative, 1-low, 2-medium, 3-strong) and percentage of stained cells (0%-0%, 1%-1%-25%, 2%-25%-50%, 3%-50%-100%). The final evaluation results were obtained by adding the staining intensity score and the percentage score, 3 points or less was regarded as SLC25A22 low expression, and 4 points or more was considered as SLC25A22 high expression.

Reverse Transcriptase-Polymerase Chain Reaction

The TRIzol reagent was used to isolate total RNA from frozen tissue samples and cultured cells. Reverse transcriptase-polymerase chain reaction (RT-PCR) was performed on the RNA reverse-transcribed cDNA using SYBR Premix Ex Taq (Takara, China). The SLC25A22 primers, Forward-GCTGCCGGA CAGAAGTGG, Reverse-CATTGATGAGCTTGGCTGGC, were used in this study, with GAPDH used as an endogenous control gene. SLC25A22-shRNA sequences (CCGGCATCG CACAGGTGGTCTACTTCTCGAGAAGTAGACCACCT GTGCGATGTTTTTGG) were provided.

Cell Counting Kit-8 Assay

Cell proliferation was measured using the cell counting kit-8 (CCK-8) kit (Dojindo Laboratories, Japan). The treated cells were collected and inoculated into 96-well plates at a density of

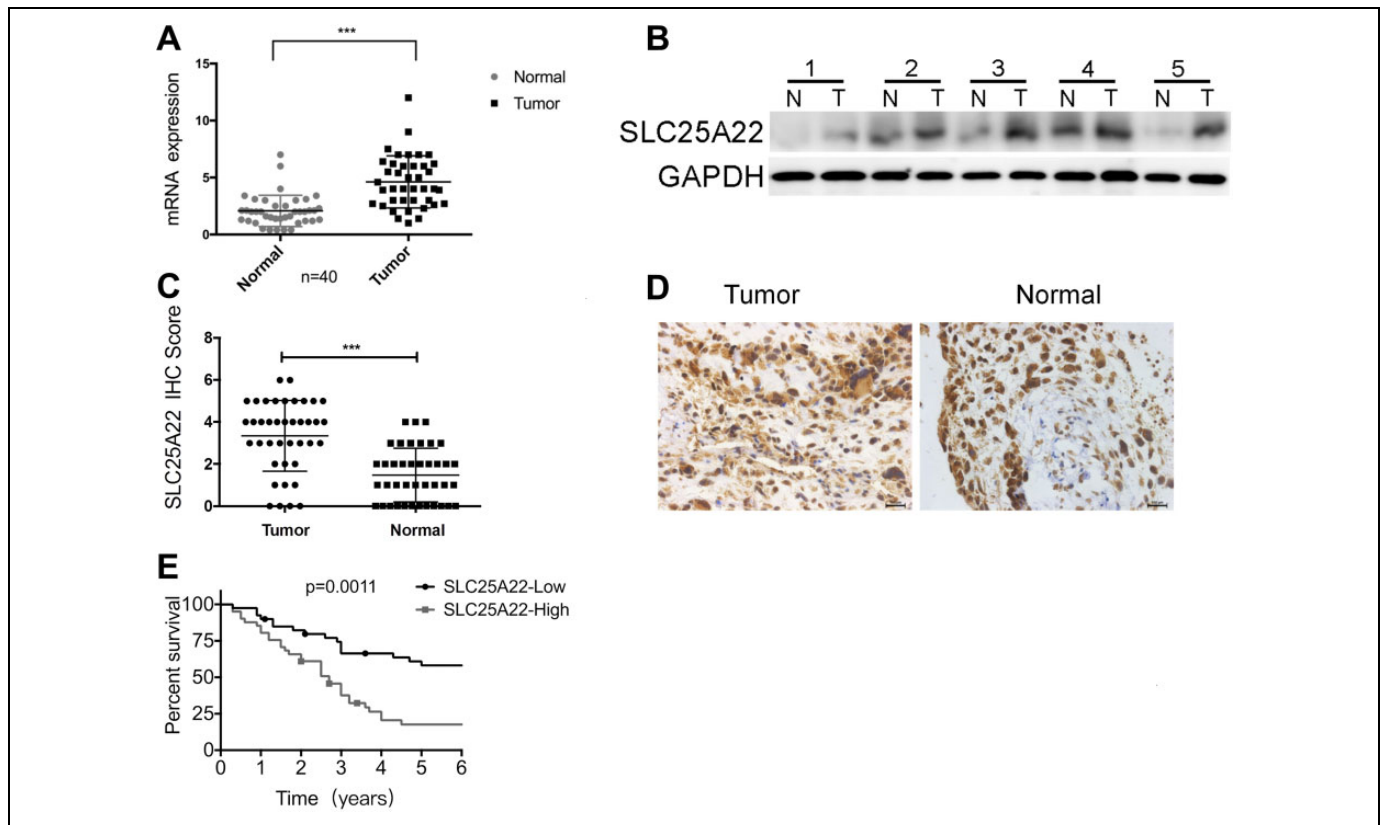


Figure 1. SLC25A22 is highly expressed in human osteosarcoma. A, The total RNA of 40 osteosarcoma tissues and their adjacent tissues was extracted, and SLC25A22 mRNA was detected by RT-PCR. B, The protein of 40 osteosarcoma tissues and their adjacent tissues was extracted and the protein level of SLC25A22 was detected by Western blot. C, The expression of SLC25A22 in osteosarcoma tissues and paracancerous tissues was detected by IHC. D, A typical IHC schematic showing the expression of SLC25A22 in osteosarcoma tissues and adjacent tissues. E, Survival curve of patients with osteosarcoma expressing SLC25A22 at high and low levels. IHC indicates immunohistochemical; RT-PCR, Reverse transcriptase-polymerase chain reaction.

10^4 cells per well and cultured for 24 to 72 hours. Then, 10 μ L of CCK-8 solution was added to each well at 24, 48, and 72 hours, and cell viability was measured using a microplate reader at 450 nm absorbance.

Colony Formation Assay

Treated cells were seeded into 12-well plates with 100 cells per well, then cultured at 37°C for approximately 15 days. The cells on the plate were washed twice with phosphate buffer saline (PBS) solution and fixed with 4% paraformaldehyde for 30 minutes, before the addition of 500 μ L of crystal violet for 15 minutes. Colonies were counted and statistically analyzed.

Cell Cycle Assay

The cell cycle assay was performed using 4×10^6 treated cells, which were collected and fixed at 4°C in 70% ethanol overnight. The cells were then resuspended in PBS and incubated with 10 mg/mL RNase and 1 mg/mL propidium iodide for 30 minutes at 37°C. DNA content analysis was performed by flow cytometry (BD Biosciences, USA). Modfit software was used to analyze the distribution of cells in different stages of the cell cycle.

Cell Apoptosis Assay

In brief, 2×10^6 osteosarcoma cells were inoculated in 6-well plates. After digestion to collect cells, cells were stained with Annexin V-FITC and PE-PI (Sigma-Aldrich, USA) in the dark for 5 minutes. Finally, the proportion of apoptosis was quantified by flow cytometry on a flow cytometer (BD Biosciences, USA).

Xenograft Tumor Model and Lung Metastasis Model in Vivo

Subcutaneous transplantation of tumors was achieved by implanting 4×10^6 Saos-2 cells into the skin of BALB/c nude mice. The length and width of the tumor was measured every other week to determine the tumor volume. The mice were sacrificed at 35 days and the tumors were extracted and weighed. The lung metastasis model was established by injecting the treated 5×10^6 Saos-2 cells into the BALB/c mice via the tail vein. The mice were sacrificed 30 days later to observe the metastases of the osteosarcoma cells in the lungs and statistically analyzed. All experiments were approved by the First Affiliated Hospital of Zhengzhou University Ethics Committee.

Wound Healing Assay

Equal amounts of differently treated cells were seeded in 6-well plates to approximate confluence, linear wounds were carefully made with 200 μ L sterile tips, cell debris was removed by washing with PBS, and cells were incubated for 24 hours. Photographs of the wound monolayer were taken at 0 and 24 hours after wounding.

Cell Invasion Assay

To measure cell invasion, a Transwell (Corning Incorporated) was placed in the well of a 24-well culture plate. In the lower chamber, 600 μ L of DMEM medium containing 10% fetal bovine serum was added, with serum-free DMEM and treated 10^5 cells added to the upper chamber. After 24 hours of culture, the migrated cells were fixed with 4% paraformaldehyde and stained with 0.1% crystal violet. The number of cells was quantified by counting 3 independent fields under a light microscope.

TdT-mediated dUTP Nick-End Labeling (TUNEL) Assay

The treated Saos-2 cells were fixed in 4% paraformaldehyde for 30 minutes, washed once with PBS and incubated with 0.1% Triton X-100 in an ice bath for 2 minutes. The treated cells were then washed twice with PBS, 50 μ L of TUNEL solution (Roche, 11684817910) was added and the cells were incubated at 37°C for 60 minutes. Finally, the cells were observed under a fluorescence microscope.

Statistical Analysis

The SPSS version 17.0 was used for all statistical analyses. All experimental data are expressed as mean (SD) of at least 3 independent experiments. The *t* test was used to analyze the differences between the experimental groups. Kaplan-Meier survival analysis was performed to analyze survival distribution. Spearman correlation analysis was used to assess the correlation between the expression levels of SLC25A22 and clinical data. All differences were considered statistically significant at $P < .05$.

Results

High Expression of SLC25A22 in Human Osteosarcoma

The RT-PCR results showed that the mRNA level of *SLC25A22* was highly expressed in osteosarcoma tissues compared to adjacent tissues (Figure 1A). Similarly, SLC25A22 protein was highly expressed in tumor tissues (Figure 1B). The immunohistochemical (IHC) analysis of SLC25A22 expression in 40 pairs of tissue specimens showed that SLC25A22 is significantly higher expressed in osteosarcoma tissue than paracancerous tissue (Figure 1C and D). These 40 tumor tissues were further divided into a high-expression group and low-expression group according to IHC scores, the results showed

Table 1. Analysis of SLC25A22 Expression and Clinical Data of Patients With Osteosarcoma.

Variables	Cases (n)	SLC25A22 Expression		P Value
		Low	High	
Total	40	16	24	
Age (years)				.930
<20y	27	10	17	
\geq 20y	13	5	8	
Gender				.692
Male	24	9	15	
Female	16	7	9	
Histology				.501
Osteoblastic	17	6	11	
Chondroblastic	13	4	9	
Fibroblastic	7	4	3	
Others	3	2	1	
Tumor location				.777
Distal femur	23	10	13	
Proximal tibia	13	5	8	
Elsewhere	4	1	3	
Ennecking staging				.0011
I/II	17	12	2	
III/IV	23	10	13	
Distant metastases				.003
No	14	10	4	
Yes	26	6	20	

that SLC25A22 was closely related to the patient's ennecking stage and distal metastasis ($P < .05$, Table 1). Moreover, the survival of osteosarcoma patients with a high expression of SLC25A22 was significantly lower than that of patients with low SLC25A22 expression (Figure 1E). These results indicate that SLC25A22 is highly expressed in human osteosarcoma tissues and predicts a poor prognosis.

Increased Proliferation of Osteosarcoma Cell Lines by SLC25A22 In Vitro and In Vivo

Next, it was found that SLC25A22 is highly expressed in U2OS and Saos-2 cells, with lower expression in HOS cells (Figure 2A). Therefore, U2OS, Saos-2, and HOS cells were selected as research models, with shRNA knockdown of *SLC25A22* gene performed in U2OS and Saos-2 cells, and SLC25A22 overexpressed in HOS cells (Figure 2B). Knockdown and overexpression of SLC25A22 in osteosarcoma cells were then detected at both mRNA (Figure 2C) and protein levels (Figure 2B). In U2OS and Saos-2 cells, knockdown of SLC25A22 by shRNA significantly slowed cell proliferation. In HOS cells, overexpression of SLC25A22 increased the proliferation rate of cells (Figure 2D). Similarly, colony formation assays confirmed that the number of clones in SLC25A22 knockdown U2OS and Saos-2 cells was reduced, and the number of clones of HOS cells was increased by SLC25A22 overexpression (Figure 2E). Then, the functions of SLC25A22 were investigated in *in vivo* tumors. Subcutaneous tumorigenesis experiments were performed in nude mice with stably

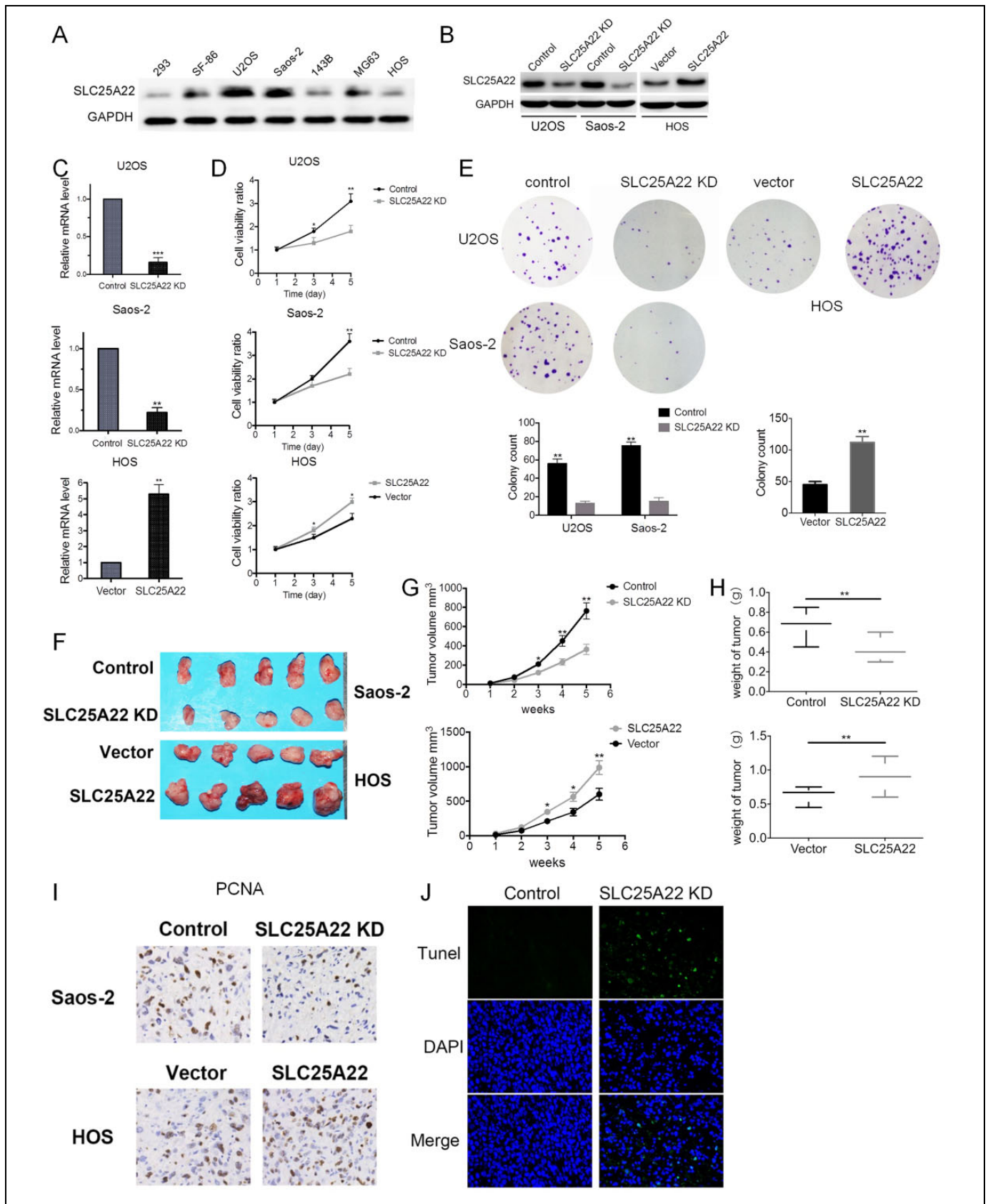


Figure 2. SLC25A22 increases proliferation of osteosarcoma cell lines in nude mice models. A, 293, SF-86, U2OS, Saos-2, 143B, MG63, HOS cells were lysed and SLC25A22 protein levels were detected by Western blot. B, SLC25A22 knockdown efficiency and overexpression were detected by Western blot. C, The knockdown and overexpression efficiency of SLC25A22 was examined by RT-PCR. D, SLC25A22 KD U2OS

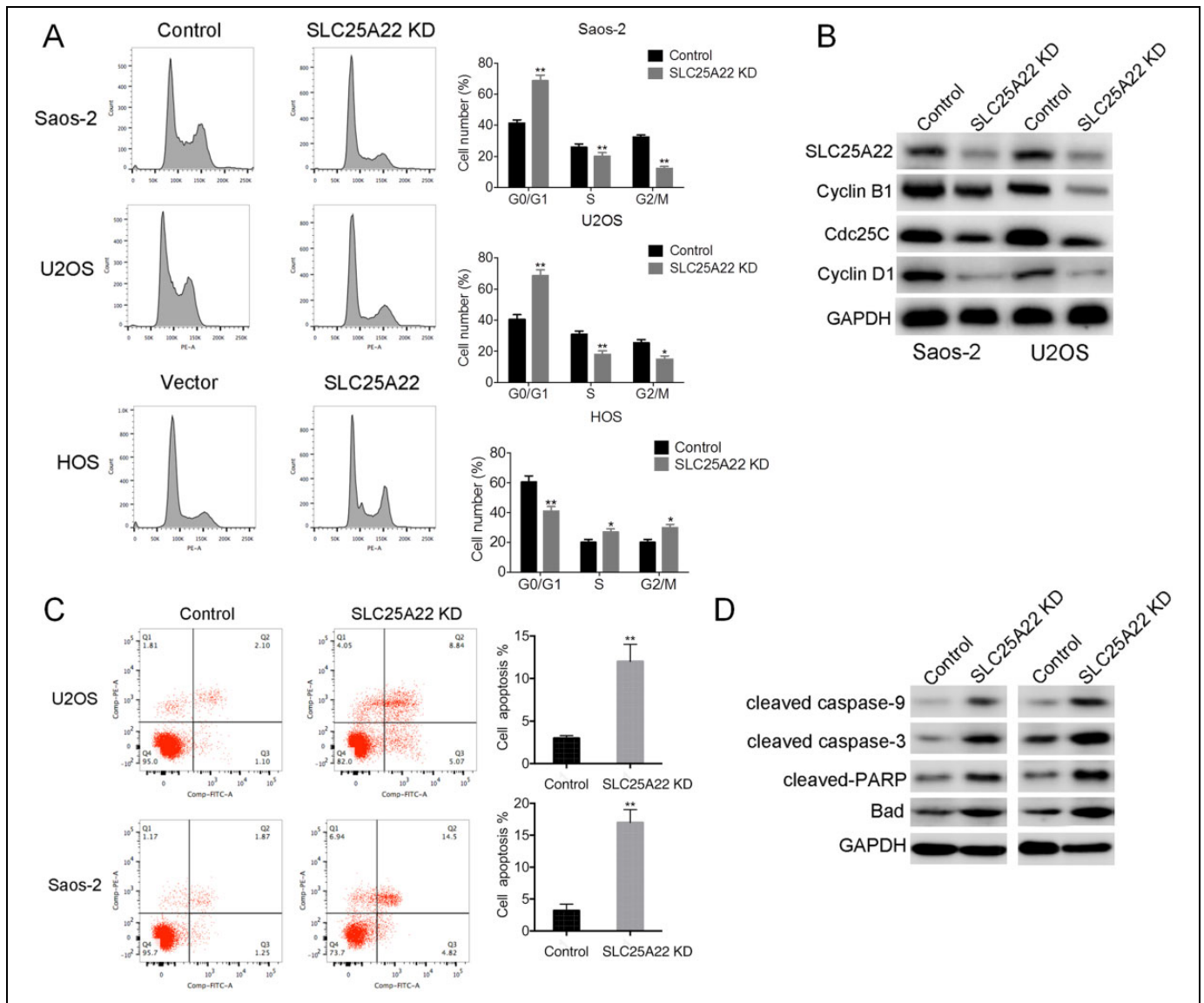


Figure 3. SLC25A22 accelerates cell cycle progression and inhibits cell apoptosis of osteosarcoma cells. A, SLC25A22 KD U2OS, Saos-2 cells and overexpressing HOS cells were subjected to cell cycle detection by flow cytometry. The results were analyzed with Modifit software and the proportions for each period were calculated. B, SLC25A22, cyclin B1, cdc25c, and cyclin D1 protein levels were detected by Western blot in SLC25A22 KD U2OS, Saos-2 cells and overexpressing HOS cells. C, Forty-eight hours after U2OS and Saos-2 cells were transfected with shRNA (SLC25A22 KD or control), cells were stained with FITC-Annexin V and PE-PI, and apoptotic cells were detected by flow cytometry and subsequently analyzed with *Flowjo* software. D, Cleaved caspase-3, cleaved caspase-9, cleaved PARP, and Bad were detected by Western blot in SLC25A22 KD U2OS, Saos-2 cells and overexpressing HOS cells.

expressing SLC25A22-shRNA Saos-2 cells and stably overexpressing SLC25A22 HOS cells. The tumor forming ability of SLC25A22 knockdown Saos-2 cells was significantly

reduced (Figure 2F), with the tumor size (Figure 2G) and weight (Figure 2H) being significantly smaller than those of the control group. In contrast, the HOS cell tumorigenicity,

Figure 2. (Continued). and Saos-2 cells and overexpressing HOS cells were cultured in 96-well plates, and the number and viability of the cells were respectively measured using CCK-8 after 1, 2, and 3 days of culture. E, SLC25A22 KD U2OS and Saos-2 cells and overexpressing HOS cells were subjected to colony formation experiments, and the number of clones was recorded. F, Saos-2 cells and HOS cells were infected with lentivirus containing SLC25A22-shRNA and SLC25A22 overexpression vector, respectively. Stably infected Saos-2 cells and HOS cells were implanted subcutaneously in nude mice. After 3 weeks, the tumor was removed and photographed. G, During tumor growth, the tumor volume was recorded. H, At the end of the experiment, the tumor weight of each group was measured. I, After the above-mentioned grouped tumor tissues were embedded in paraffin, the expression of PCNA was detected by immunohistochemistry. J, The tumor paraffin sections were subjected to the TUNEL assay, and green fluorescence represented tissue cells with DNA damage.

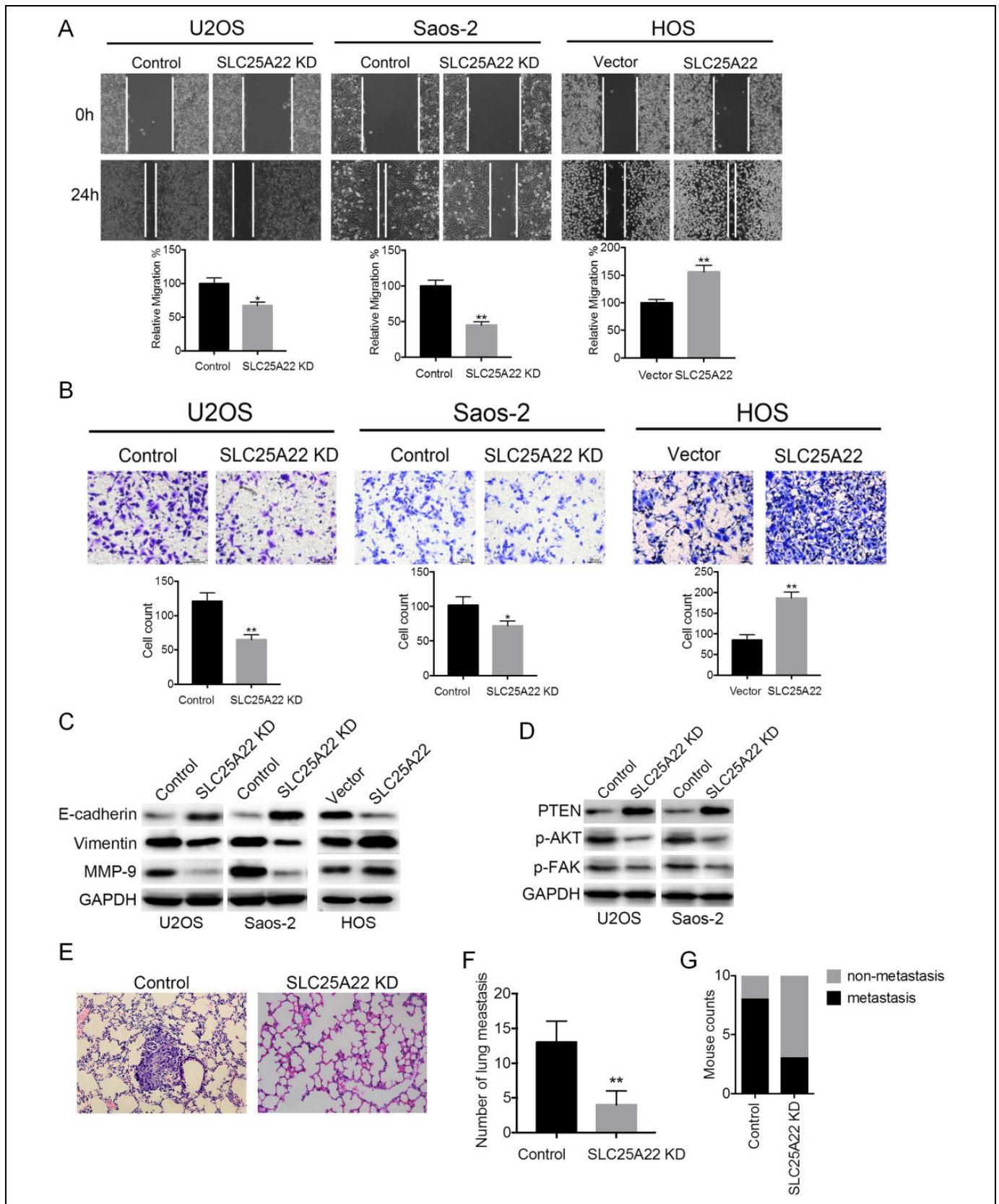


Figure 4. A, SLC25A22 promotes the invasion and metastasis of osteosarcoma cells by altering the PTEN signaling pathway. Wound healing assay: stable SLC25A22 knockdown U2OS, Saos-2 cells, and overexpressed HOS cells were plated in 6-well plates for wound healing experiments, and healing was observed and photographed at 24 hours. B, Cell invasion assay: stable SLC25A22 knockdown U2OS, Saos-2 cells,

tumor volume, and weight increased after SLC25A22 overexpression (Figure 2F-H). Immunohistochemistry of SLC25A22-knockdown and overexpressed tumor tissues showed that the expression of proliferating cell nuclear antigen (PCNA) was significantly reduced after SLC25A22 knockdown, and increased after SLC25A22 overexpression (Figure 2I). Immunofluorescence staining showed that apoptosis-induced DNA damage was significantly increased in SLC25A22-knockdown tumor tissues by TUNEL assay (Figure 2J). These results indicated that SLC25A22 promoted the proliferation of osteosarcoma cell lines and tumor formation in nude mice models.

Acceleration of Cell Cycle Progression and Suppression of Cell Apoptosis by SLC25A22 in Osteosarcoma Cells

Compared to the control group, the G0/G1 phase ratio of SLC25A22 knockdown U2OS and Saos-2 cells was increased, and the ratio of S phase and G2/M phase was decreased, indicating that SLC25A22 knockdown inhibited cell cycle progression. In contrast, the ratio of G0/G1 phase in the cell cycle of HOS cells overexpressing SLC25A22 was decreased, and the ratio of S and G2/M phases was increased (Figure 3A). The expression of cell cycle-related proteins was examined before and after SLC25A22 intervention. After SLC25A22 knockdown in U2OS and Saos-2 cells, the expression of cyclin B1, cdc25c, and cyclin D1 was significantly decreased (Figure 3B). The expression of SLC25A22 was also associated with inhibition of apoptosis in osteosarcoma cells. SLC25A22 knockdown in osteosarcoma cell lines U2OS and Saos-2 resulted in a significant increase in the proportion of apoptotic cells compared to the control group (Figure 3C). When cells are in apoptosis, caspase-3, caspase-9, and PARP will be cleaved, which can be used as a marker of apoptosis. There was a significant increase in the expression of cleaved caspase-3, cleaved caspase-9, and cleaved PARP as well as an increase in the expression of apoptosis-related protein Bad after SLC25A22 knockdown in U2OS and Saos-2 cells (Figure 3D). In summary, SLC25A22 could accelerate the progression of osteosarcoma cell cycle and inhibit osteosarcoma cell apoptosis.

Promotion of the Invasion and Metastasis of Osteosarcoma Cells Attributed to SLC25A22 Altering the PTEN Signaling Pathway

In the wound healing assay, the migration ability of U2OS and Saos-2 cells after SLC25A22 knockdown was decreased, while HOS cell migration speed after SLC25A22 overexpression was

increased (Figure 4A). In Transwell experiments, U2OS and Saos-2 cells after SLC25A22 knockdown reduced cell invasion, and HOS cells increased after SLC25A22 overexpression (Figure 4B). Epithelial to mesenchymal transition (EMT) promotes invasion and metastasis of tumor cells. E-cadherin inhibits this process, whereas vimentin and MMP-9 promotes EMT. The expression of E-cadherin in SLC25A22 knockdown U2OS and Saos-2 cells increased, with a decreased expression of vimentin and MMP-9, whereas overexpression of SLC25A22 caused the opposite in HOS cells (Figure 4C). The PTEN signaling pathway participates in this process, as knockdown of SLC25A22 reduced PTEN expression and increased phosphorylation of Akt and FAK (Figure 4D). Next, the Saos-2 cells knocked down by SLC25A22 were injected into nude mice via the tail vein to establish a metastatic model of osteosarcoma cells. The HE staining showed that the control group of osteosarcoma cells metastasized in the lung, while the lung metastasis cells were significantly reduced after SLC25A22 knockdown (Figure 4E and 4F). Furthermore, the proportion of lung metastases after SLC25A22 knockdown was significantly reduced (Figure 4G). Based on the above results in cell lines and mice model, we hypothesize that SLC25A22 promoted the invasion and metastasis of osteosarcoma by regulating the PTEN signaling pathway.

Discussion

It is well known that SLC25A22 encodes a high-capacity mitochondrial glutamate carrier expressed in cells with increased metabolic demands.^{25,26} There is growing evidence that metastatic lesions may encounter more oxidative stress than primary tumors, therefore requiring the upregulation of the tricarboxylic acid cycle (TCA) cycle intermediates.²⁷ Studies have shown that high expression of SLC25A22, which encodes the mitochondrial glutamate transporter in other tumors, alters the production of mitochondria-associated metabolic pathways and metabolites, including amino acid metabolism such as alanine and aspartic acid, and the ornithine cycle.²⁴ After interference with the tumor suppressor PTEN, the glutamate transporter-mediated increase in glutamate metabolism is enhanced, while inhibition of PTEN inhibits the proteasomal degradation pathway of glutamate transporters.²⁸ Therefore, the promotion of SLC25A22 in osteosarcoma may also depend on the PTEN-mediated glutamate metabolic pathway.

It has been shown that SLC25A22 is a novel oncogene in KRAS-mutant colorectal cancer. SLC25A22 knockdown inhibits cell growth and migration/invasion in KRAS-mutant colorectal cancer cells *in vitro*, attenuating

Figure 4. (Continued). and overexpressed HOS cells were plated in Transwells and the invaded cells were stained with crystal violet and photographed. C, E-cadherin, vimentin, and MMP-9 protein levels were detected by Western blot in SLC25A22 knockdown U2OS, Saos-2 cells, and overexpressed HOS cells. D, PTEN, phosphorylated Akt, and phosphorylated FAK were detected by Western blot in SLC25A22 knockdown U2OS, Saos-2 cells, and overexpressed HOS cells. E, Control and SLC25A22 knockdown Saos-2 cells were used to construct a lung metastasis model, and HE staining showed 2 groups of lung metastases. F, Comparison of the number of lung metastatic cells in the control and SLC25A22 knockdown groups. G, The number of mice with lung metastases in the two groups, control and SLC25A22 knockdown lung metastasis model mice.

tumorigenicity and metastasis *in vivo*.²³ This study was the first to demonstrate that SLC25A22 promotes the proliferation and metastasis of osteosarcoma cells by regulating the PTEN signaling pathway, and is significantly correlated with the poor prognosis of patients with osteosarcoma. Downregulation of SLC25A22 significantly inhibited the proliferation of osteosarcoma cell lines, increased the apoptosis of osteosarcoma cell lines and significantly increased cells in G0/G1 phase. Transwell experiments confirmed that the downregulation of SLC25A22 significantly decreased the invasion and migration of osteosarcoma cells. Studies have shown that the positive expression rate of PTEN in osteosarcoma is significantly lower than that in cartilage tissue, suggesting that the expression of the PTEN protein is decreased in osteosarcoma, thus losing the negative regulation of cell cycle, causing abnormal proliferation of cells and leading to tumorigenesis.²⁹ The molecular biology of PTEN regulation in osteosarcoma is mainly the mutation or heterozygous deletion of the *PTEN* gene. The protein encoded by the *PTEN* gene can negatively regulate the PI3K/Akt signal transduction pathway in osteosarcoma, antagonizing this signal pathway to inhibit the pathological process of the tumor.³⁰ The Western blotting data showed that the expression of the PTEN protein in osteosarcoma cell lines was significantly increased after SLC25A22 expression was inhibited. Therefore, SLC25A22 can regulate the biological behavior of osteosarcoma cells by inhibiting PTEN.

Epithelial to mesenchymal transition is a critical step in the invasion metastasis cascade.³¹⁻³³ This study showed that SLC25A22 induced EMT phenotypes in osteosarcoma cells by activating mesenchymal markers and downregulating epithelial markers. In addition, knockdown of SLC25A22 reduces the expression of MMP9, which plays an important role in the formation of the tumor microenvironment and in the promotion of cancer progression and metastasis.³⁴ However, the mechanism by which SLC25A22 regulates EMT and MMPs needs further exploration.

Metastatic cancer cells undergo significant metabolic rewiring and this metabolic plasticity allows them to survive under restricted conditions.³⁵⁻³⁷ The present study shows that the metabolic enzyme SLC25A22 promotes the invasion and metastasis of osteosarcoma. Mechanistically, the PTEN signaling pathway is involved in role of SLC25A22 in the invasion and metastasis of osteosarcoma. These findings suggest that the SLC25A22/PTEN pathway is a new mechanism for osteosarcoma metastasis, so PTEN inhibitors may be useful for treating patients with osteosarcoma with high SLC25A22 expression.

Authors' Note

The protocol was approved by the Ethic Committee of First Affiliated Hospital of Zhengzhou University (ID=2015-LW-034). Ming-Wei Chen is also affiliated with Orthopedics department, Zhengzhou Orthopedics Hospital Affiliated to Henan University, Zhengzhou, Henan province, China.


Declaration of Conflicting Interests

The author(s) declared no potential conflicts of interest with respect to the research, authorship, and/or publication of this article.

Funding

The author(s) received no financial support for the research, authorship, and/or publication of this article.

ORCID iD

Xue-jian Wu, PhD  <https://orcid.org/0000-0003-3750-8054>

References

1. Wu J, Sun H, Li J, et al. Increased survival of patients aged 0-29 years with osteosarcoma: a period analysis, 1984-2013. *Cancer Med*. 2018;7(8):3652-3661.
2. Berner K, Johannesen TB, Berner A, et al. Time-trends on incidence and survival in a nationwide and unselected cohort of patients with skeletal osteosarcoma. *Acta Oncol*. 2015;54(1):25-33.
3. Pruksakorn D, Phanphaisarn A, Pongnikorn D, et al. AgeStandardized incidence rates and survival of osteosarcoma in northern Thailand. *Asian Pac J Cancer Prev*. 2016;17(7):3455-3458.
4. Marina N, Gebhardt M, Teot L, Gorlick R. Biology and therapeutic advances for pediatric osteosarcoma. *Oncologist*. 2004;9(4):422-441.
5. Chou AJ, Geller DS, Gorlick R. Therapy for osteosarcoma: where do we go from here? *Paediatr Drugs*. 2008;10(5):315-327.
6. Tan ML, Peter FM, Dass CCR. Osteosarcoma: conventional treatment vs. gene therapy. *Cancer Biol Ther*. 2009;8:106-117.
7. Ta HT, Dass CR, Choong PF, Dunstan DE. Osteosarcoma treatment: state of the art. *Cancer Metastasis Rev*. 2009;28(1-2):247-263.
8. Ganjavi H, Gee M, Narendran A, et al. Adenovirus-mediated p53 gene therapy in osteosarcoma cell lines: sensitization to cisplatin and doxorubicin. *Cancer Gene Ther*. 2006;13(4):415-419.
9. Chou AJ, Gorlick R. Chemotherapy resistance in osteosarcoma: current challenges and future directions. *Expert Rev Anticancer Ther*. 2006;6(7):1075-1085.
10. Park HR, Jung WW, Bertoni F, et al. Molecular analysis of p53, MDM2 and H-ras genes in low. *Pathol Res Pract*. 2004;200(6):439-445.
11. Hu X, Yu AX, Qi BW, et al. The expression and significance of IDH1 and p53 in osteosarcoma. *J Exp Clin Cancer Res*. 2010;29:43.
12. Lau CC. Molecular classification of osteosarcoma. *Cancer Treat Res*. 2009;152:459-465.
13. Zhang F, Li M, Wu X, et al. 20(S)-ginsenoside Rg3 promotes senescence and apoptosis in gallbladder cancer cells via the p53 pathway. *Drug Des Devel Ther*. 2015;9:3969-3987.
14. Glen H, Mason S, Patel H, Macleod K, Brunton VG. E7080, a multi-targeted tyrosine kinase inhibitor suppresses tumor cell migration and invasion. *BMC Cancer*. 2011;11:309.
15. Raftopoulos M, Etienne-Manneville S, Self A, Nicholls S, Hall A. Regulation of Cell Migration by the C2 domain of the tumor suppressor PScience TEN. *Science*. 2004;303(5661):1179-1181.

16. Gildea JJ, Herlevsen M, Harding MA, et al. PTEN can inhibit in vitro organotypic and in vivo orthotopic invasion of human bladder cancer cells even in the absence of its lipid phosphatase activity. *Oncogene*. 2004;23(40):6788-6797.
17. Carver BS, Tran J, Gopalan A, et al. Aberrant ERG expression cooperates with loss of PTEN to promote cancer progression in the prostate. *Nat Genet*. 2009;41(5):619-624.
18. Li J, Yen C, Liaw D, et al. PTEN a putative tyrosine phosphatase gene mutated in human brain, breast, and prostate cancer. *Science*. 1997;275(5308):1943-1947.
19. Ma J, Sawai H, Ochi N, et al. PTEN regulates angiogenesis through PI3K/Akt/VEGF signaling pathway in human pancreatic cancer cells. *Mol Cell Biochem*. 2009;331(1-2):161-171.
20. Gong T, Su X, Xia Q, Wang J, Kan S. Expression of NF-kappaB and PTEN in osteosarcoma and its clinical significance. *Oncol Lett*. 2017;14(6):6744-6748.
21. Fiermonte G, Palmieri L, Todisco S, Agrimi G, Palmieri F, Walker JE. Identification of the mitochondrial glutamate transporter. Bacterial expression, reconstitution, functional characterization, and tissue distribution of two human isoforms. *J Biol Chem*. 2002;277(22):19289-19294.
22. Casimir M, Lasorsa FM, Rubi B, et al. Mitochondrial glutamate carrier GC1 as a newly identified player in the control of glucose-stimulated insulin secretion. *J Biol Chem*. 2009;284(37):25004-25014.
23. Wong CC, Qian Y, Li X, et al. SLC25A22 promotes proliferation and survival of colorectal cancer cells with KRAS mutations, and xenograft tumor progression in mice, via intracellular synthesis of aspartate. *Gastroenterology*. 2016;151(5):945-960.e6.
24. Li X, Chung ACK, Li S, et al. LC-MS-based metabolomics revealed SLC25A22 as an essential regulator of aspartate-derived amino acids and polyamines in KRAS-mutant colorectal cancer. *Oncotarget*. 2017;8(60):101333-101344.
25. Poduri A, Heinzen EL, Chitsazzadeh V, et al. SLC25A22 is a novel gene for migrating partial seizures in infancy. *Ann Neurol*. 2013;74(6):873-882.
26. Molinari F, Kaminska A, Fiermonte G, et al. Mutations in the mitochondrial glutamate carrier SLC25A22 in neonatal epileptic encephalopathy with suppression bursts. *Clin Genet*. 2010;76(2):188-194.
27. Johnson CH, Dejea CM, Edler D, et al. Metabolism links bacterial biofilms and colon carcinogenesis. *Cell Metabolism*. 2015;21(6):891-897.
28. Yang L, Wang S, Sung B, Lim G, Mao J. Morphine induces ubiquitin-proteasome activity and glutamate transporter degradation. *J Biol Chem*. 2008;283(31):21703-21713.
29. Tian K, Di R, Wang L. MicroRNA-23a enhances migration and invasion through PTEN in osteosarcoma. *Cancer Gene Ther*. 2015;22(7):351-359.
30. Li T, Xiao Y, Huang T. HIF1alpha-induced upregulation of lncRNA UCA1 promotes cell growth in osteosarcoma by inactivating the PTEN/AKT signaling pathway. *Oncol Rep*. 2018;39(3):1072-1080.
31. Zeisberg M, Neilson EG. Biomarkers for epithelial-mesenchymal transitions. *J Clin Invest*. 2009;119(6):1429-1437.
32. Zhang F, Xiang S, Cao Y, et al. EIF3D promotes gallbladder cancer development by stabilizing GRK2 kinase and activating PI3K-AKT signaling pathway. *Cell Death Dis*. 2017;8(6):e2868.
33. Zhang F, Ma Q, Xu Z, et al. Dihydroartemisinin inhibits TCTP-dependent metastasis in gallbladder cancer. *J Exp Clin Cancer Res*. 2017;36(1):68.
34. Shay G, Lynch CC, Fingleton B. Moving targets: Emerging roles for MMPs in Cancer Progression and Metastasis. *Matrix Biol*. 2015;44-46:200-206.
35. Gill JG, Piskounova E, Morrison SJ. Cancer, oxidative stress, and metastasis. *Cold Spring Harb Symp Quant Biol*. 2017;81:163-175.
36. Kroemer G, Pouyssegur J. Tumor cell metabolism: cancer's achilles' heel. *Cancer Cell*. 2008;13(6):472-482.
37. Teoh ST, Lunt SY. Metabolism in cancer metastasis: bioenergetics, biosynthesis, and beyond. *Wiley Interdiscip Rev Syst Biol Med*. 2017;10(2):e1406.